MECHANICAL PROPERTY ISSUES FOR GEOTHERMAL WELL CEMENTS

A.J. Philippacopoulos and M.L. Berndt
Department of Energy Sciences and Technology
Brookhaven National Laboratory

Geothermal Resources Council Transactions, Vol. 25, 119-124, San Diego, 2001

ABSTRACT

This paper addresses material requirements for cements used in geothermal wells. The approach taken combines laboratory tests with engineering finite element analysis of typical cased and cemented geothermal wellbore. It is shown that the usual design approach, which is based on compressive strength requirements, is inadequate. Development of cements with enhanced tensile strength as well as appropriate testing for defining respective failure loads is needed in future studies.

INTRODUCTION

Traditional design guidelines for geothermal well cements require maintenance of compressive strength of at least 1,000 psi (6.9 MPa) and permeability less than 0.1 milliDarcy throughout downhole exposure of 12 months (API Task Group, 1985). In terms of mechanical properties and overall well integrity, these guidelines are very limited. There is a need to consider other properties, i.e., Young's modulus, Poisson's ratio, tensile and shear strength. The results of the present study show that the latter properties influence the response of the cement due to pressure and temperature loads encountered in a geothermal well. Therefore, the adequacy of deciding whether a cement design is acceptable based on its compressive strength is questionable. This applies to analysis of cements in existing wells as well as the development of new cement formulations for future use. The limitations of solely relying on the compressive strength of the cement have also been raised in recent studies of oil and gas wells (Bosma et al., 1999). The present study raises similar concerns for geothermal wells.

Brookhaven National Laboratory (BNL) has been conducting research on the behaviour and required mechanical properties of patch cements used to remediate deformed well casing (Philippacopoulos and Berndt, 2000; 2001). This work has shown the importance of cement to withstand the tensile stresses developed by internal pressurization and thermal effects. The same general principle applies to conventional cemented geothermal wells in that structural integrity depends on properties other than compressive strength. Combination of experimental characterization of different cement types with finite element analysis to evaluate the ability of these cements to withstand operational stresses will lead to improved cement design criteria so that optimal well life is achieved.

EXPERIMENTAL PROCEDURE

Plain and fibre reinforced cements were tested for mechanical properties. The plain cements have been subjected to uniaxial and triaxial compression, tensile, flexural and thermal property

tests. To date, the fibre reinforced cements have been screened for tensile strength and the results will be presented in the future. In this paper results for a standard Class G cement/40% silica flour mix (40SF), a latex-modified mix (40SFL), and a perlite-modified mix (40SFP) are presented. More details on the properties and testing procedure for the plain cements are available elsewhere (Philippacopoulos and Berndt, 2000; 2001).

Selected plain cement formulations were tested in uniaxial and triaxial compression at elevated temperature (200°C, 392°F). Ambient temperature tests under uniaxial conditions were also conducted for comparison. The specimens had a diameter of 38 mm and length of 76 mm. For the elevated temperature tests it was necessary to use a low confining pressure of 100 psi. Static elastic modulus and Poisson's ratio in compression were determined under the same conditions. Triaxial compression tests were conducted on the standard and latex-modified cements with pore pressure of 300 psi and confining pressures of 1,000, 2,000 and 3,000 psi. Two specimens per confining pressure were tested for each mix. All specimens subjected to elevated temperature tests were vacuum saturated with 1M NaCl solution to simulate geothermal brine. The uniaxial and triaxial compression tests were performed in a stiff, servocontrolled testing machine in order to follow the post-peak portion of the stress-strain curves. Splitting tensile strength at ambient temperature was measured in accordance with ASTM C 496 on six cylinders 76 mm diameter and 145 mm long.

EXPERIMENTAL RESULTS AND DISCUSSION

The stress-strain curves for the unmodified Class G/40% silica flour (40SF) and latex-modified cements (40SFL) at ambient temperature are given in Figure 1 and the companion results at elevated temperature are shown in Figure 2. Figure 1 indicates the brittle behaviour of the unmodified cement. While the latex-modified cement can also be classified as brittle, the stress-strain curve shows a greater degree of strain-softening in the post-peak region and some residual strength after post-peak deformation. The decrease in peak strength and elastic modulus with addition of latex is also apparent. Both materials exhibited linear elastic behaviour up to approximately 50% of the peak stress. The stress-strain curve for the unmodified mix at 200°C (Figure 2) lacks smoothness. Once again, the unmodified cement is brittle whereas the mix containing latex shows strain-softening in the post-peak region. Although not smooth, the post-peak region is generally less steep for the latex-modified cement when tested at 200°C and the residual strength is higher.

The results of the triaxial compression tests on the unmodified and latex-modified cements at elevated temperature are summarized in the form of stress-strain curves in Figure 3. The unmodified cement shows a drop after the peak stress to a residual strength. This contrasts with behaviour under uniaxial conditions. The peak stress and peak strain increase as the confining pressure is increased. For the latex-modified cement the behaviour is more ductile, particularly at confining pressures of 2,000 and 3,000 psi where strain-hardening is extensive. Post-peak strain softening and residual strength are only observed at 1,000 psi confining pressure. Thus, the brittle-ductile transition pressure lies between 1,000 and 2,000 psi. Comparison between the stress-strain curves indicates the ability of latex to impart ductility to the well cement. Furthermore, Mohr-Coulomb plots were constructed and the angle of internal friction (Φ) and

coefficient of linear cohesion (c) were 28.9^o and 2654 psi for the unmodified cement. Addition of latex changed Φ to 20.4^o and c to 1558 psi.

The elastic properties determined under uniaxial conditions at 200°C and the ambient temperature tensile strengths are summarized in Table 1. Preliminary tests on fibre reinforced cements have shown that tensile strengths up to 1109 ± 29 psi can been achieved an ongoing research is examining how this can be improved further. The influence of temperature on tensile strength will also be investigated.

Table 1. Elevated Temperature Elastic Properties and Ambient Tensile Strengths of Cements

Mix Code	Elastic Modulus (x 10^6 psi)	Poisson's Ratio	Tensile Strength (psi)
40SF	1.46 ± 0.09	0.18 ± 0.05	755 ± 12
40SFL	0.96 ± 0.01	0.18 ± 0.02	670 ± 87
40SFP	0.87 ± 0.01	0.17 ± 0.01	376 ± 45

MODELLING APPROACH

The magnitude of the stress in the cement depends on: (a) properties of cement; (b) properties of the casing; (c) properties of the formation; (d) far-field stresses at the site of the well; and, (e) amplitude and the distribution of the expected loads during the lifetime of the well. Other factors include the geometry of the configuration and the conditions at the casing/cement and cement/formation interfaces. Usually, such interfaces are assumed to be of the welded type, i.e., both stress and deformations are considered to be continuous across the interface. However, due to potential debonding, a more realistic modelling i.e., using Coulomb friction interface elements in the finite element model is more appropriate.

The pressure response problem simulated by our 2D finite element models is defined as follows: the pressure is prescribed within a circular hole representing the interior of a cased geothermal well. Referring to a $O(x_1,x_2,x_3)$ Cartesian system (x_3 axis perpendicular to x_1,x_2 plane), the stresses σ_{11}, σ_{22} at infinity are prescribed. The latter represent the far-field compressive stress regime in the region, which is generally orthotropic. Similar conditions apply in the thermal stress analysis except that the temperature is prescribed in the interior of the well and also at the free-field. For the pressure problem, an ideal case involving two concentric rings surrounded by an infinite medium has been tackled analytically (Atkinson and Eftaxiopoulos, 1996) for both in-plane and out-of-plane conditions. Their model, although valuable for preliminary assessments, it is overly simple, thus difficult to use it in more real applications.

The two sides of the one-quarter finite element 2D model were subjected to appropriate displacement boundary conditions to ensure symmetry in the deformed shape. P/T loads were applied at the inner boundary, which was left to deform freely. Different considerations were given to the outer boundary. One of them was to leave it free thus simulating a zero stress condition or to allow for application of prescribed far-field stresses. We also experimented with zero displacements to see how the stresses/deformations within the borehole are affected by assuming either zero stress or zero displacement conditions at the outer boundary. These

considerations were valuable in selecting where to place geometrically the outer boundary of the model so that we simulate semi-infinite conditions, which are in accordance with the physics of the problem. Constraining the model appropriately was critical to performing pressure and thermal stress analysis. Finally, in the heat conduction analysis the temperature was prescribed in the inner boundary while the outer boundary was assigned a far-field temperature. In terms of size, 2D models incorporated 1292 nodes and 1206 elements.

PRESSURE AND THERMAL STRESS ANALYSIS

Stresses due to Well Pressure

The stress field due to internal pressure was evaluated using 2D plane strain finite element models. The internal pressure was set at 200 psi. Two key parametric variations were considered in the pressure response analysis of geothermal wells. First, the material of the surrounding formation was taken to be the same, then softer and finally stiffer than that of the cement. Second, while the internal pressure at the geothermal well was kept constant at 200 psi, the far-field stress was varied as follows: (a) zero; (b) 100 psi and (c) 300 psi. The radial stress (normalized to the applied pressure) due to the internal pressure is shown in Figure 4(a) for all parametric variations considered in the analysis. Results for radial distances up to ten times the inner radius of the geothermal well were evaluated. From Figure 4(a) it can be seen that the radial stress is compressive for all cases considered. At low R/R_o values, the dimensionless radial stress tends to unity while at high R/R_o values the dimensionless radial stress tends to the ratio of the far-field stress to the applied stress (i.e., zero, 0.5 and 1.5 respectively). The corresponding dimensionless tangential stresses are shown in Figure 4(b). Note that the circumferential stresses can be either tensile or compressive depending on: (a) the far-field stress; and, (b) the ratio between the Young's modulus of the cement to that of the surrounding rock.

From Figure 4(b) it can be seen that in the absence of far-field compressive stress, the cement is most likely to develop radial cracks and fail in tension due to the circumferential stresses. The effect of the Young's modulus ratio is not relevant at this stage. However, when the far-field stresses increase, this ratio becomes critical. From Figure 4(b), by observing the three curves at low R/R_o values which correspond to the cement (the interface between cement/rock is at R/R_o =3.14) it can be concluded that stiffer cements result in higher circumferential stresses. This is also true for the radial stress. For example, by comparison of the stress curves shown in Figure 4(a) within the low R/R_o range it can be clearly seen that cements characterized by higher Young's modulus (as compared to the surrounding rock) result in higher radial stresses.

Finally, by considering the results from both radial and circumferential stresses at higher far-field stresses shown in Figure 4, it can be concluded that in the presence of compressive far-field stresses the cement is likely to fail in shear. This seems to be the predominant failure mode when the cement is stiffer than the formation. When the cement is less stiff than the formation such shear failure is minimized. Our material tests discussed in the previous section revealed that test cements flow plastically in compression and known plasticity models such as Mohr-Coulomb or the Willam-Warnke model can be used in the finite element analysis. Standard tension-cut-off or smeared cracking models can be used for the same purpose. It is important,

however, to realize that although the far-field compressive stress at the site can reduce the tensile tangential stresses in the cement, that reduction is associated with some level of uncertainty. Accordingly, cement sealants are likely to be subjected to tensile tangential stresses due to internal pressure. Because cements are inherently low tensile strength materials a systematic effort is needed to enhance the tensile strength of such materials for application to geothermal wells (Philippacopoulos and Berndt, 2000; 2001).

Thermal Stresses

A steady-state heat conduction simulation was carried out using 2D finite element analysis. The temperature at the interior of the geothermal well was set at 450°F. A far-field temperature of 55.4 ^{o}F was assumed for the analysis. The nodal temperatures from the heat conduction were subsequently input to perform thermal stress analysis. Again, the ratio of the Young's modulus of the rock to that of the cement was treated parametrically as was done in the pressure stress analysis described in the previous section. The radial thermal stress as function of R/R_o is plotted in Figure 5(a) for the different Young's modulus ratios considered in the analysis. As expected, the radial stresses for all cases converge to zero in the interior of the geothermal well. As the rock becomes harder than the cement, we see kinks in the variations of radial stress with R/R_o. Such kinks are developed at the cement/formation interface due to the resulting mismatch in material properties. Note, however, that the curves in Figure 5(a) are continuous since continuity at all interfaces was assumed throughout the analysis. Temperature effects due to gaps at similar interfaces have been studied in Philippacopoulos and Berndt (in press).

Finally, as shown in Figure 5(a), radial stresses from all cases considered tend to zero at high R/R_o values. This assumption was made by the thermal stress analysis. By comparing the three curves of Figure 5(a) within the region R/R_o <3.14 (cement sealant area), it can be seen that the softer cement is subjected to higher compressive radial stresses. On the other hand, although stiffer cements are subjected to lower radial stresses, they are also associated with tensile circumferential stresses (at about 500 psi) as can be observed from Figure 5(b). Therefore, for both loading conditions (internal pressure as well as temperature) tensile cracking failure is possible to occur if the cement is stiffer than the rock. Strictly speaking, however, the issue of soft versus stiff cements should not be addressed in a generic sense. The above results demonstrate that it is a problem-specific issue.

CONCLUSIONS

Engineering analysis of the stress field in geothermal wells due to pressure and temperature loading leads to the following conclusions:

- Stresses at the cement depend strongly on: (a) the far-field stress at the site of the well; and, (b) on the stiffness contrast between cement and formation.

- The basic failure modes of the cement in a geothermal wellbore are: (a) tensile failure in the absence of compressive far-field stresses; and, (b) shear failure in the presence of compressive far-field stresses.

- The issue of stiff versus soft cements cannot be addressed generically. It is a problem-specific issue.

- In both thermal and pressure loads when the probable mode of failure is a tensile one, then stiffer cements attract higher tensile stresses than soft cements.

Although the compressive far-field stress can have a relieving impact on the cement stresses, there are associated uncertainties (i.e., interface conditions, cyclic changes of in-situ stresses). Consequently, it is recommended that designs of cements for geothermal wells must require a level of tensile strength. Improvement of tensile strength is being addressed in current research on fibre reinforced materials. Failure stresses need to be investigated by first improving our knowledge of failure criteria of cements for geothermal applications. This in turn would require more data to define failure surfaces, which subsequently can be used to perform nonlinear analysis.

ACKNOWLEDGEMENTS

This work was supported by the U.S. Department of Energy Office of Wind and Geothermal Technologies and performed under contract number DE-AC02-98CH10886. The program manager was Ray LaSala. The elevated temperature and triaxial compression testing was performed by TerraTek, Inc. and the assistance of Roberto Suarez-Rivera is appreciated.

REFERENCES

C. Atkinson and D.A. Eftaxiopoulos, A Plane Model for the Stress Field Around an Inclined, Cased and Cemented Wellbore, International Journal for Numerical and Analytical Methods in Geomechanics, Vol. 20, pp. 549-569, 1996.

API Task Group on Cements for Geothermal Wells, API Work Group Reports Field Tests of Geothermal Cements, Oil and Gas Journal, February 11, pp. 93-97, 1985.

M. Bosma, K Ravi, W. van Driel and G.J. Schreppers, Design Approach to Sealant Selection for the Life of the Well, SPE 56536, 1999.

A.J. Philippacopoulos and M.L. Berndt, Characterization and Modeling of Cements for Geothermal Well Casing Remediation, Geothermal Resources Council Transactions, Vol. 24, 81-86, San Francisco, 2000.

A.J. Philippacopoulos and M.L. Berndt, Influence of Debonding in Ground Heat Exchangers Used with Geothermal Heat Pumps, Geothermics, in press.

A.J. Philippacopoulos and M.L. Berndt, Engineering Analysis of Materials for Remediation of Geothermal Wells, BNL Informal Report, April 2001.

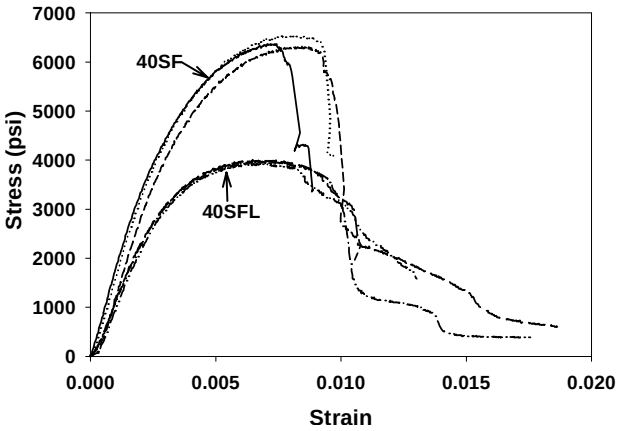

Figure 1. Uniaxial compression stress-strain curves for cements at ambient temperature.

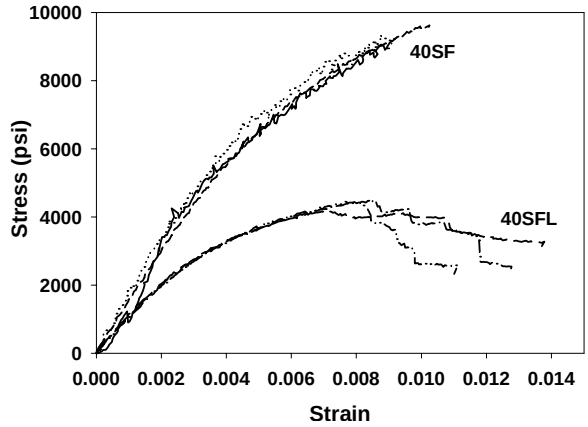

Figure 2. Uniaxial compression stress-strain curves for cements at elevated temperature.

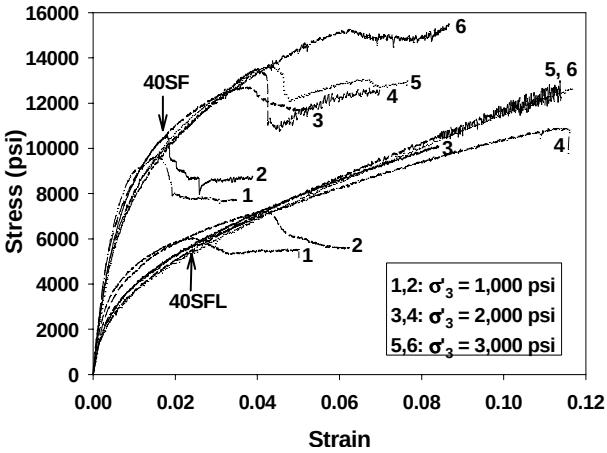

Figure 3. Triaxial compression stress-strain curves for cements at elevated temperature.

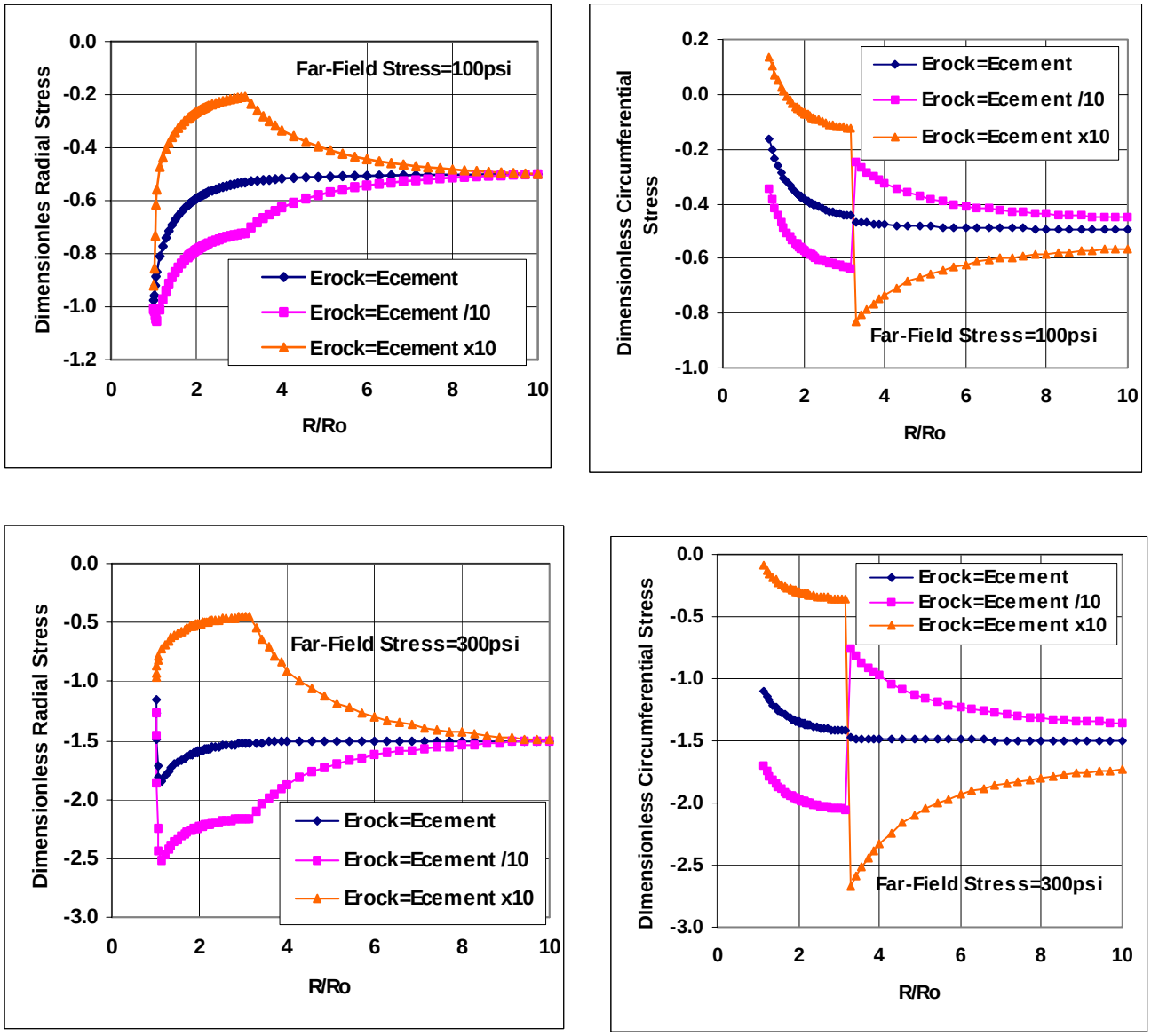

(a) (b)

Figure 4. Pressure stress variations: (a) radial and (b) tangential.

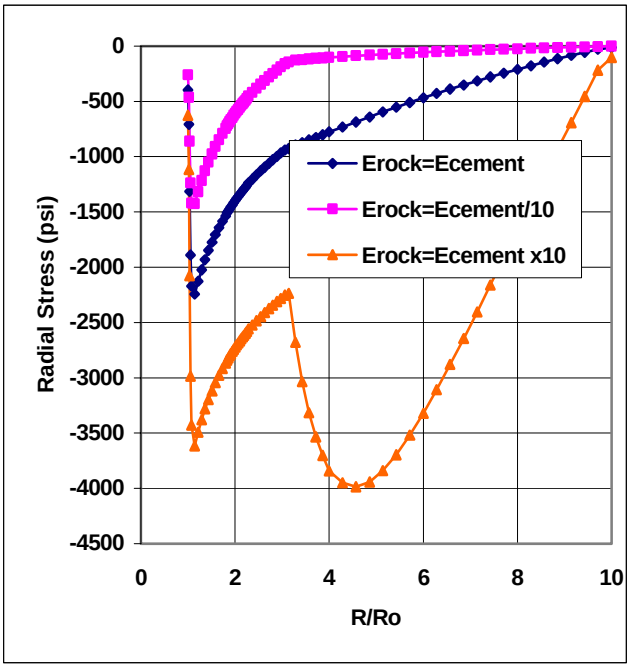

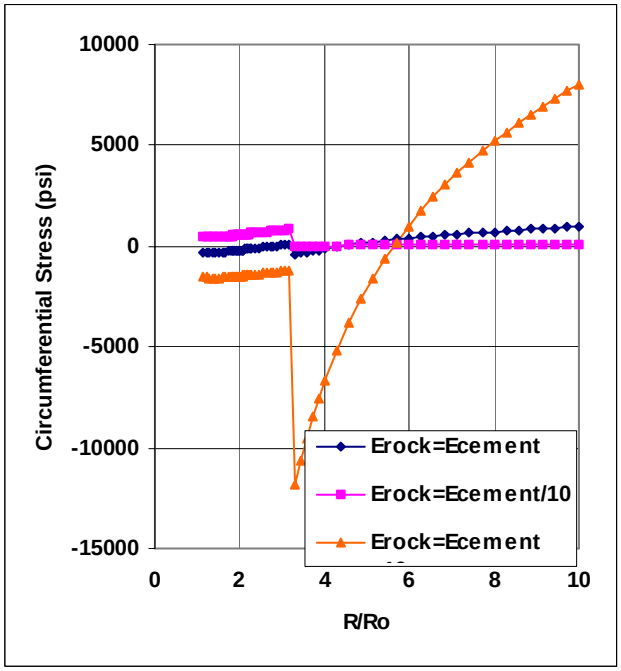

(a) (b)

Figure 5. Thermal stress variations: (a) radial and (b) tangential.